Bioactive Materials 4 (2019) 17–21

Contents lists available at ScienceDirect

Bioactive Materials

journal homepage: http://www.keaipublishing.com/biomat

A facile fabrication of novel stuff with antibacterial property and osteogenic promotion utilizing red phosphorus and near-infrared light

Bo Huang[a,1], Lei Tan[a,1], Xiangmei Liu[a,*], Jun Li[b], Shuilin Wu[a,b,**]

[a] Ministry-of-Education Key Laboratory for the Green Preparation and Application of Functional Materials, Hubei Key Laboratory of Polymer Materials, School of Materials Science & Engineering, Hubei University, Wuhan, 430062, China

[b] School of Materials Science & Engineering, The Key Laboratory of Advanced Ceramics and Machining Technology by the Ministry of Education of China, Tianjin University, Tianjin, 300072, China

ARTICLE INFO

Keywords:
Implants
Red phosphorus
Near-infrared
Osteogenesis
Antibacterial
Biofilm

ABSTRACT

Bone-implant materials are important for bone repairing and orthopedics surgery, which include bone plates and bone nails. These materials need to be designed not only considering its biostability and biocompatibility, but also their by-products induced infection after therapy or long-time treatment *in vivo*. Thus, the development of novel implant materials is quite urgent. Red phosphorus has great biocompatibility and exhibits efficient photothermal ability. Herein, a red phosphorus/IR780/arginine-glycine-asparticacid-cysteine (RGDC) coating on titanium bone-implant was prepared. The temperature sensitivity of *Staphylococcus aureus* biofilm is enhanced in the presence of ROS produced by IR780 with 808 nm light irradiation. With keeping the cells and tissues normal, a high antibacterial performance can be realized by near-infrared (808 nm) irradiated within 10 min at 50 °C. Besides the high effective antibacterial efficacy provided by photothermal therapy (PTT) and photodynamic therapy (PDT), the RGDC decorated surface can also possess an excellent performance in osteogenesis *in vivo*.

1. Introduction

Since artificial bone implants had been developed from decades ago, researchers have made great efforts to design novel biomaterials because these materials can be widely used in fractures fixation, dental implant and orthopedics surgery [1]. Implant-associated infections (IAIs) that often occur in bone implant surgery or later period therapy is a serious complication, which makes patients anguished and demands repeated surgery with costly treatment [2]. The reason of IAIs occurred was the failed internal fixation or the formation of highly resistant biofilm after infection, which makes it difficult to achieve effective antibiotic concentration in local tissues of the lesion [3,4]. Thus, optimal methods for the prophylaxis may be taken into account. One strategy is to design artificial materials that contain components to destruct biofilm; the other way is to develop engineered surface with anti-infective and immuno-enhancement properties.

Photothermal therapy (PTT) or photodynamic therapy (PDT) performed by near-infrared (NIR) light [5], has been attracting many researchers due to their potential antibacterial performance. In addition, these two kinds of treatments exhibit excellent performance for their strong penetration to human body and the fewer side effects. For killing bacteria, PTT (808 nm NIR) requires photothermal agents to transform optical energy into local heat [6]. Several explored materials have been utilized in antibacterial applications, such as some noble metal nanoparticles, semiconductor nanorods, and other organic compounds. The primary problem to overcome is that the antibacterial efficacy can reach over 90% only in the condition of around 85 °C. However, this quite excessive temperature can disrupt nature tissues and lead to other diseases or problems [7,8]. A mass of works have confirmed that reactive oxygen species (ROS) such as $^1O_2$ can kill bacteria by destroying its protein or DNA [9–11]. By combining photosensitizer, a relevant light can stimulate material to produce ROS and kill bacteria. However, the hypoxic environment will limit the PDT efficiency *in vivo* due to the lower ROS yields, which is a great challenge for PDT in the future [12,13].

Phosphorus is a vital element containing in the human body,

Peer review under responsibility of KeAi Communications Co., Ltd.

* Corresponding author.

** Corresponding author. Ministry-of-Education Key Laboratory for the Green Preparation and Application of Functional Materials, Hubei Key Laboratory of Polymer Materials, School of Materials Science & Engineering, Hubei University, Wuhan, 430062, China.

E-mail addresses: liuxiangmei1978@163.com (X. Liu), shuilinwu@tju.edu.cn (S. Wu).

[1] The two authors contribute to this work equally.

https://doi.org/10.1016/j.bioactmat.2018.11.002
Received 26 October 2018; Received in revised form 17 November 2018; Accepted 17 November 2018
Available online 23 November 2018

occupying 1% of the total body weight. Recent study disclosed that as an allotrope of phosphorus, red phosphorus (RP) has been proved to be nontoxic even long-term existence in human body because the degradation of RP is biocompatible [14]. Moreover, RP is much cheaper than black phosphorus [14,15].

In this paper, we reported that a Ti-RP-IR780-RGDC bone implant shows good biostability and biocompatibility with excellent antibacterial property under NIR irradiation. With the synergistically effect of photothermal effect at a low temperature of 50 °C by RP and ROS produced by IR780 using 808 nm laser, the biofilm could be eradicated *in vivo*. In addiction, the osteogenic ability could be enhanced by RGDC, which makes it possible to apply in clinical orthopedics.

2. Experimental

2.1. Materials preparation

Medical-grade pure Ti plates (6 mm diameter, 2 mm thick) and rods (2 mm diameter, 6 mm thick) were purchased from Fu-Tai Metal Materials Co. (China). Red phosphorus (RP) was purchased from Sinopharm Chemical Reagent Co. (China), IR780 was purchased from Sigma-Aldrich (USA), and RGDC peptide was purchased from GL Biochem (Shanghai) Ltd.

RP is a material with amorphous structure, IR780 functions as a photosensitizer to generate ROS and RGDC is a peptide which works for promoting osteogenesis.

Medical-grade pure Ti with a diameter of 6 mm and a thickness of 2 mm was used for the substrates. The plates were treated with polishing beforehand and then cleaned in mixture of organic solvents by a ultrasonic cleaner to remove contaminants.

To remove the impurity from the surface of RP, 6 g of commercial RP was added into 40 mL H_2O and hydrothermally treated in an autoclave at a temperature of 200 °C for a whole night. After that, the reactor was cooled until it turned to room temperature, and the treated RP was washed several times with water and then stoved for further use.

The processed RP powders were placed tidily in a porcelain box, and Ti plates were placed in a tube furnace followed. The tube furnace was inflated with Ar gas, then, the heating temperature parameters was set and kept at the temperature of 650 °C for 5 h and 350 °C for 2 h, respectively. By the end of the reaction, the tube furnace was chilled naturally to room temperature. The product was stored in an argon atmosphere.

As a final step, first, 10 μL of a dichloromethane solution of IR780 (0.02 mg/mL) was dripped onto the surface of the Ti-RP plates then dried. To obtain polydopamine (PDA) modified Ti-RP-IR780, the samples of Ti-RP-IR780 were soaked in dopamine hydrochloride in Tris-HCl buffer (pH 8.5) for a day at 25 °C. The samples were washed by deionized water and dried. Then, the samples were immersed in a 2 mg/mL RGDC peptide in PBS (pH 7.4) for 24 h at room temperature. The excess RGDC was wiped off by deionized water, finally, the target product of Ti-RP-IR780-RGD was obtained after drying in vacuo [15].

2.2. Structure characterization

The surface morphologies of Ti-RP were examined by scanning electronic microscopy (SEM, JSM-6510LV, JEOL, Japan). Transmission electron microscopy (TEM) images of RP were obtained using a Tecnai G20 transmission electron microscope (USA).

2.3. Detection of ROS

The generation of ROS from the IR780 could be evaluated by microplate reader (SpectraMax i3, Molecular Devices). (1,3-diphenylisobenzofuran) DPBF was used as a ROS detector to measure the ROS produced from Ti, Ti-RP (50 °C), Ti-RP-IR780-RGDC (25 °C) and Ti-RP-IR780-RGDC (50 °C), then these four groups were illuminated by the 808 nm laser in a proper intensity for 60 s (recorded every 10 s for 6 times).

2.4. Evaluation of the photothermal performance of Ti-RP-IR780-RGDC in vivo

To determine the thermal conversion efficiency that Ti-RP-IR780-RGDC contained, then the samples soaked in DI H_2O were irradiated under 808 nm laser light with a intensity of 0.5 W/cm^2. The temperature was recorded by an thermal imager (FLIR Systems Inc, USA, MSX Resolution: 320 × 240; thermal sensitivity: < 0.05 °C; temperature range: −20 to 650 °C; accuracy: ± 2 °C) every 10 s.

2.5. In vivo assay of animal bone-implantation

All of the experiments to the animals were obtained permission from the Hubei Provincial Centers for Disease Prevention & Control. Some adult male white rats weighing around 450 g were used in the experiments. The rats were arranged into two groups: Ti and Ti-RP-IR780-RGDC. These rats were anaesthetized with chloral hydrate (10%, 4 mL/kg) prior before surgery and placed on sterile gauzes during surgery. The two groups of rats were implanted into the tibia closed to the knee joint and labeled. After implantation, the incision was sutured charily. After the surgery, the rats were located into individual cages and raised under the same condition. After two days, the two squads were treated by the 808 nm laser (0.5 W/cm^2). After 14 days, the rats were euthanized with excess chloral hydrate.

2.6. Spread plate analysis

To identify the growth of bacteria *in vivo*, the rods of two groups were removed from the shank and rolled on culture medium and then placed at a temperature of 37 °C for one day to observe the growth of the bacterial colonies.

2.7. Histological analysis

The soft tissue and bone around the implants were treated in paraformaldehyde and cleaned by EDTA. The infectious soft tissues around the implants were cut and immersed in a formaldehyde solution at a refrigerating layer for 3 days, then washed with PBS, and finally infiltrated with ethanol. Then, hematoxylin and eosin (H & E) and Van Gieson's picro fuchsin staining was performed after a month. The images were captured on a fluorescence microscope (IFM, Olympus, IX73).

2.8. Micro-CT evaluation

Four weeks after surgery, the tibias from each group were taken into 2D scanning in a computed tomography (CT, SkyScan 1176), system with a scanning time of 300 ms (60 kV and 400 μA). The 2D high-resolution reconstructed images were obtained from the software provided by the CT manufacturer.

2.9. Static analysis

Every test was evaluated as mean values ± standard deviation of several independent measurements. A one-way analysis of variance (ANOVA) program and a student t-test was accepted to estimate the statistical significance of the variance. The values of $^{**}P < 0.01$ were regarded as statistically significance.

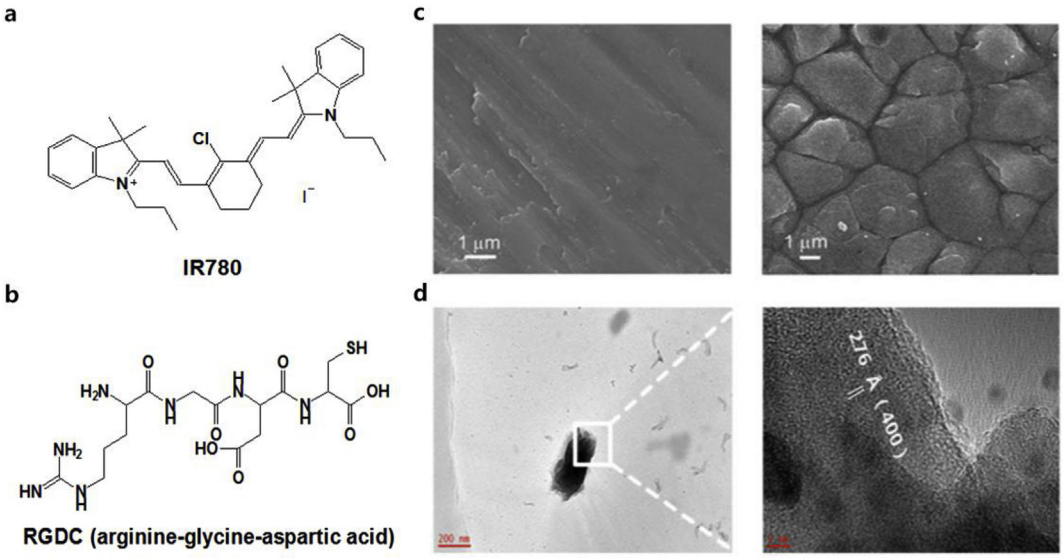

Fig. 1. The chemical formula of (a) IR780, and (b) RGDC, (c) SEM images of Ti-RP. (d) TEM image of RP separated from Ti-RP, the scale bar fixed with 200 nm and 5 nm, respectively.

3. Results and discussion

3.1. Surface and microstructure characterization

SEM images disclosed the surface morphologies of the RP film on the Ti plate (Fig. 1c). Obviously, the Ti-RP showed the structure of uniform polyhedra. The TEM images of the RP separated from Ti-RP was shown in Fig. 1d. The parallel lattice fringes of the (400) facets with a d-spacing of 2.76 Å were emerged clearly, which confirmed that there was a fibrous red phosphorus coating created on the substrate [15].

3.2. ROS monitor and analysis

Fig. 2a shows the ROS-generating curve of Ti, Ti-RP (50 °C), Ti-RP-IR780-RGDC (25 °C), and Ti-RP-IR780-RGDC (50 °C) with irradiation by 808 nm laser. The absorbance of DPBF in Ti-RP-IR780-RGDC (25 °C) and Ti-RP-IR780-RGDC (50 °C) were quite similar. Both groups were notably lower than that of the Ti and Ti-RP (50 °C) groups, proving that the ROS could be triggered by the additive IR780, and whether at the temperature of 50 °C or 25 °C had little obviously influence on the photosensitizer of IR780.

3.3. Photothermal properties of Ti-RP-IR780-RGDC

The 808 nm laser is considered as one of the best suitable NIR wavelengths for PTT due to its high depth of skin penetration and low absorbance by the tissues in body. As demonstrated in Fig. 2b, under the laser irradiation, the temperature risen to 120 °C in 80 s and descended to 30 °C within 120 s for the first cycle, and the data exhibited similarly in the second and third cycle. As reported previously [15], there was no photothermal quality in IR780 or RGDC, therefore it could be indicated that RP was an efficient photothermal material and could provide a condition for utilizing in PTT.

3.4. In vivo antibacterial ability

The growth of bacteria was shown in Fig. 3a, only a little bacterial colonies can be viewed on the plate in the group of modification. For comparison, the bacterial colonies in Ti + light group were rather countless. From the consequence exhibited in culture medium, it indicated that the antibacterial activity of Ti-RP-IR780-RGDC + Light is much better than the group of Ti + Light.

In addition, to further study the tissues, H&E staining was used. The results were obtained by H & E staining shown in Fig. 3b–c. By comparing the number of inflammatory cells, the Ti + light group shows abundant while the Ti-RP-IR780-RGDC + light group appears little,

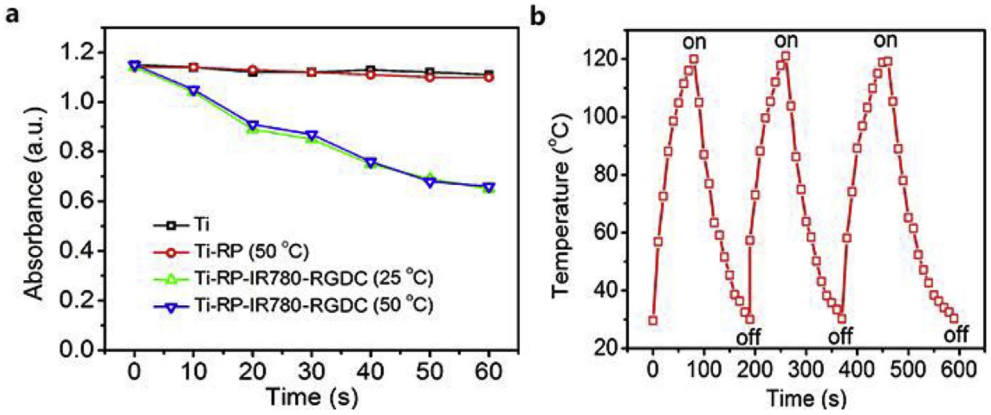

Fig. 2. (a) ROS detection of Ti, Ti-RP(50 °C), Ti-RP-IR780-RGDC(25 °C), Ti-RP-IR780-RGDC(50 °C). (b) Cycle heating curve of Ti-RP-IR780-RGDC.

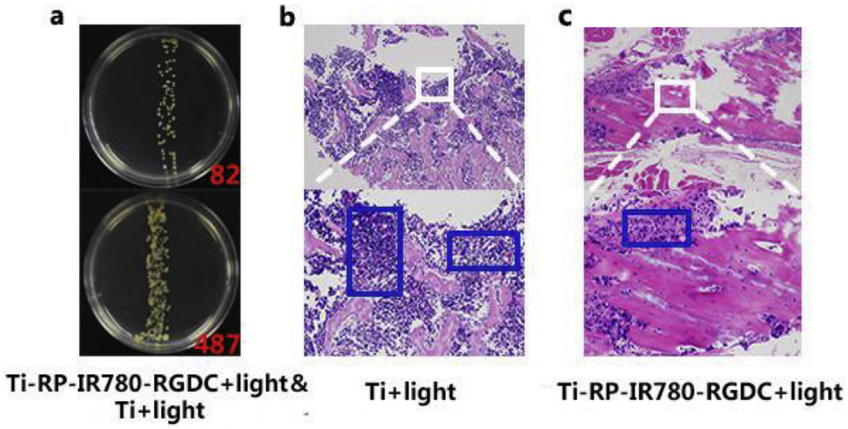

Fig. 3. (a) Photograph of bacteria colonies and culture mediums of Ti + Light and Ti-RP-IR780-RGDC + Light rods taken from rats. (b,c) H&E staining images show tissue infection degree of rats treated by samples.

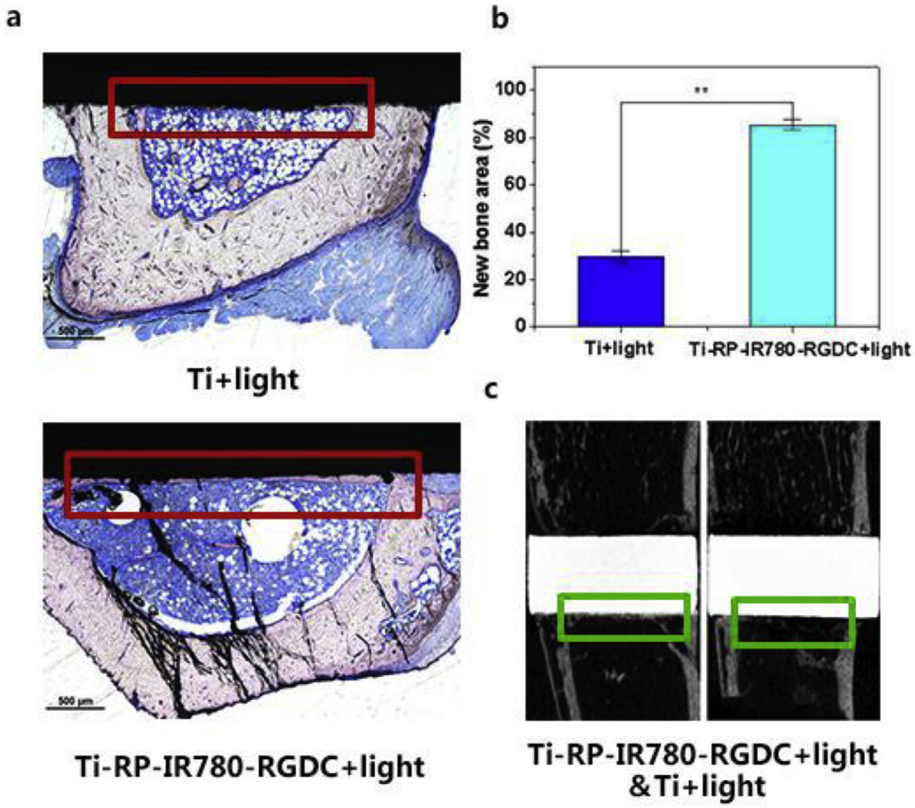

Fig. 4. (a) Histological characteristics at the Bone-implant interfaces stained with Van Gieson's picro fuchsin (scale bars = 500 μm); (b) Percentage of new bone area (**P < 0.01); (c) Micro-CT images of the coronal sections.

which indicated that Ti-RP-IR780-RGDC + Light implantation had no obvious infection *in vivo*.

3.5. Histopathological and Micro-CT evaluation

The newly formed bone was stained by Van Gieson's picro fuchsin and examined by Micro-CT. In the image of tibia section (Fig. 4a), it exhibited different growing states of the area of new bone formation (highlights in red rectangles). Consequently, it can be drawn a conclusion that the new bone volume of Ti-RP-IR780-RGDC + Light group is more than that in Ti + light group and there is no bacterial infection occurred on the newly formed bone. From Fig. 4b, the percentage of new bone area around Ti + light group is only 26.8 ± 2.51%, while the corresponding value is 85.5 ± 2.1% ($p < 0.01$) in the group of Ti-RP-IR780-RGDC + Light. In addition, the typical reconstructed central coronal sections of the implants by Micro-CT were displayed in Fig. 4c, and the new bone area was marked by green rectangles. According to the image, the bone volume around Ti-RP-IR780-RGDC + Light was bigger than that around Ti + light sample. Comparing the Ti + light and Ti-RP-IR780-RGDC + Light groups, the new bone formed a bridge connecting both sides of the medullary cavity on latter groups, which confirmed that Ti-RP-IR780-RGDC was turned out to be an effective material in promoting osteogenesis.

4. Conclusion

A facile fabrication of Ti-RP-IR780-RGDC was described, and RP was proven to be a high-performance photothermal coating using in

PTT. Also, the IR780 functions to generate ROS which shows great synergistic action to kill bacteria with combination of PTT. Furthermore, the existence of RGDC makes it possible to accelerate the osteogenesis. As the data shows, the Ti-RP-IR780-RGDC is not only confirmed to have good biostability and biocompatibility, but also shows high antibiofilm property. Furthermore, it also reveals an excellent osteogenic performance under irradiation of 808 nm laser. This bone implant with antibiofilm and osteogenic properties provides an avenue to the application of clinical orthopedics.

Acknowledgements

This work is jointly supported by the National Key R&D Program of China No. 2016YFC1100600 (sub-project 2016YFC1100604), and the National Natural Science Foundation of China, Nos. 51671081, 51871162, 51801056 and 51422102, and Natural Science Fund of Hubei Province, 2018CFA064.

References

[1] G. Jin, H. Qin, H. Cao, Y. Qiao, Y. Zhao, X. Peng, X. Zhang, X. Liu, Paul K. Chu, Zn/Ag micro-galvanic couples formed on titanium and osseointegration effects in the presence of *S. aureus*, Biomaterials 65 (2015) 22–31.

[2] J. Wang, H. Zhou, G. Guo, J. Tan, Q. Wang, J. Tang, W. Liu, H. Shen, J. Li, X. Zhang, Enhanced anti-infective efficacy of Nano-ZnO films through a combination of intrinsic anti-biofilm activity and reinforced innate defense, ACS Appl. Mater. Interfaces 39 (2017) 33609–33623.

[3] H. Cheng, W. Xiong, Z. Fang, H. Guan, W. Wu, Y. Li, Y. Zhang, M.M. Alvarez, B. Gao, K. Huo, J. Xu, N. Xu, C. Zhang, J. Fu, A. Khademhosseini, F. Li, Strontium (Sr) and silver (Ag) loaded nanotubular structures with combined osteoinductive and antimicrobial activities, Acta Biomater. 31 (2016) 388–400.

[4] J. Li, L. Tan, X. Liu, Z. Cui, X. Yang, Kelvin W.K. Yeung, Paul, K. Chu, S. Wu, Balancing bacteria-osteoblast competition through selective physical puncture and biofunctionalization of ZnO/Polydopamine/Arginine-Glycine-Aspartic Acid-Cysteine nanorods, ACS Nano 11 (2017) 11250–11263.

[5] X. Cheng, R. Sun, L. Yin, Z. Chai, H. Shi, M. Gao, Light-triggered assembly of gold nanoparticles for photothermal therapy and photoacoustic imaging of tumors *in Vivo*, Adv. Mater. 29 (2017) 1604894.

[6] B. Liu, C. Li, G. Chen, B. Liu, X. Deng, Y. Wei, J. Xia, B. Xing, P. Ma, J. Lin, Synthesis and optimization of MoS_2@Fe_3O_4-ICG/Pt(IV) nanoflowers for MR/IR/PA bioimaging and combined PTT/PDT/Chemotherapy triggered by 808 nm laser, Adv. Sci. 4 (2017) 1600540.

[7] C. He, X. Duan, N. Guo, C. Chan, C. Poon, R.R. Weichselbaum, W. Lin, Core-shell nanoscale coordination polymers combine chemotherapy and photodynamic therapy to potentiate checkpoint blockade cancer immunotherapy, Nat. Commun. 7 (2016) 12499.

[8] C. Mao, Y. Xiang, X. Liu, Z. Cui, X. Yang, Z. Li, S. Zhu, Y. Zheng, Kelvin W.K. Yeung, S. Wu, Repeatable photodynamic therapy with triggered signaling pathways of fibroblast cell proliferation and differentiation to promote bacteria-accompanied wound healing, ACS Nano 12 (2018) 1747–1759.

[9] X. Li, D. Lee, J. Huang, J. Yoon, Phthalocyanine-assembled nanodots as photosensitizers for highly efficient type I photoreactions in photodynamic therapy, Angew. Chem. Int. Ed. 57 (2018) 1–7.

[10] Z. Feng, X. Liu, L. Tan, Z. Cui, X. Yang, Z. Li, Y. Zheng, Kelvin W.K. Yeung, S. Wu, Electrophoretic deposited stable chitosan@MoS_2 coating with rapid in Situ bacteria-killing ability under dual-light irradiation, Small 14 (2018) 1704347.

[11] M. Li, X. Liu, L. Tan, Z. Cui, X. Yang, Z. Li, Y. Zheng, Kelvin W.K. Yeung, Paul K. Chu, S. Wu, Noninvasive rapid bacteria-killing and acceleration of wound healing through photothermal/photodynamic/copper ion synergistic action of a hybrid hydrogel, Biomater. Sci. 6 (2018) 2110–2121.

[12] W. Liu, T. Liu, M. Zou, W. Yu, C. Li, Z. He, M. Zhang, M. Liu, Z. Li, J. Feng, X. Zhang, Aggressive Man-made red blood cells for hypoxia-resistant photodynamic therapy, Adv. Mater. 30 (2018) 1802006.

[13] Z. Chen, M. Liu, M. Zhang, S. Wang, L. Xu, C. Li, F. Gao, Bo Xie, Z. Zhong, X. Zhang, Interfering with lactate-fueled respiration for enhanced photodynamic tumor therapy by a porphyrinic MOF nanoplatform, Adv. Funct. Mater. 28 (2018) 1803498.

[14] N.M. Latiff, W.Z. Teo, Z. Sofer, A.C. Fisher, M. Pumera, The cytotoxicity of layered black phosphorus, Chemistry 21 (2015) 13991.

[15] L. Tan, J. Li, X. Liu, Z. Cui, X. Yang, S. Zhu, Z. Li, X. Yuan, Y. Zheng, Kelvin W.K. Yeung, H. Pan, X. Wang, S. Wu, Rapid biofilm eradication on bone implants using red phosphorus and near-infrared light, Adv. Mater. 31 (2018) 1801808.